Biochimica et Biophysica Acta, 1059 (1991) 63–75

ADONIS 000527289100180U

BBABIO 43438

Stark effect spectroscopy of bacteriochlorophyll in light-harvesting complexes from photosynthetic bacteria

David S. Gottfried, Jonathan W. Stocker and Steven G. Boxer

Department of Chemistry, Stanford University, Stanford, CA (U.S.A.)

(Received 10 December 1990)

Key words: Stark effect; Electric field effect; Antenna complex; Light harvesting complex; Energy transfer

The effects of an applied electric field on the Q_y absorption and fluorescence spectra of three antenna complexes from photosynthetic bacteria have been measured at 77 K: the bacteriochlorophyll *a* protein (BCP) from *Prosthecochloris aestuarii*, the B800-850 light-harvesting complex from *Rhodobacter sphaeroides* and the B875 light-harvesting complex from *Rhodobacter capsulatus*. For BCP in a glycerol / buffer glass, the value of the change in dipole moment, $|\Delta\mu_A|$, for three of the resolved absorption bands was found to lie in the range 1.3–2.0 D/*f* (where *f* is the local field correction factor), and the Stark spectrum lineshape is well approximated by the second derivative of the absorption. This is similar to what is found for monomeric bacteriochlorophyll *a* (BChl *a*) embedded in a polymer film and for the 800 nm monomer BChl *a* band of *Rb. sphaeroides* reaction centers; thus, the BChl *a* chromophores in BCP behave largely as a non-interacting set in an electric field. For B800-850 in a glycerol / buffer glass, the BChl *a* associated with the 800 nm band has a small $|\Delta\mu_A| = 0.8$–0.9 D/*f*, while the BChl *a* of the 850 nm band is found to have $|\Delta\mu_A| = 3.1$–3.4 D/*f*; however, the Stark spectra of both components have anomalous lineshapes, which complicates the quantitative analysis. $|\Delta\mu_A|$ for the 850 nm band is nearly unchanged upon attenuation of the 800 nm band by treatment with lithium dodecyl sulfate. The Stark spectrum of the B875 complex was obtained in whole chromatophore membranes. The lineshape for B875 is also unusual, and it appears that the electrochromism is not dominated by a dipole moment change. In all three antenna complexes, efficient energy transfer occurs from higher-energy states to the lowest-energy excited state, and, at 77 K, fluorescence occurs primarily from this lowest state. The electric field modulated fluorescence of BCP shows nearly the same quantitative effect as that obtained from absorption, with $|\Delta\mu_F| = 1.6$ D/*f*. In contrast, the B800-850 complex shows an unprecedented, very large net decrease in fluorescence in an applied electric field. Possible mechanisms for this unusual result are discussed. B875 also shows an electric field induced fluorescence decrease; however, the Stark fluorescence spectrum is dominated by a first-derivative contribution, not unlike the electromodulated absorption spectrum. Explanations for this, and many of the results for strongly interacting chromophores, may lie in a breakdown of the standard treatments of electrochromism when strong intermolecular coupling dominates.

Introduction

Recent electromodulated (Stark) absorption and fluorescence experiments have demonstrated a substantial change in dipole moment for the Q_y band of the special pair bacteriochlorophyll dimer in photosynthetic reaction centers (RCs) [1–8] and certain simpler model compounds [9]. This has prompted an interest in using these same techniques to examine photosynthetic antenna complexes. Three widely studied antenna complexes spanning a range of spectral features have been selected, and results are reported for the bacteriochlorophyll *a* (BChl *a*) Q_y region of the spectrum (700–900 nm). Results from the Q_x region (400–700 nm), which are dominated by effects due to carotenoids, are reported for antenna and RC complexes in an accompanying paper [10].

Stark effect spectroscopy offers an interesting approach for probing the effects of intermolecular inter-

Abbreviations: BCP, bacteriochlorophyll *a* protein; RC, reaction center.

Correspondence: S.G. Boxer, Department of Chemistry, Stanford University, Stanford, CA 94305, U.S.A.

actions on the electronic structure of chromophores. Extensive studies of molecular crystals demonstrate that optical transitions associated with more than one chromophore often exhibit enhanced electrochromism [11–14]. At the crudest one-electron, Hückel level one expects that pure charge transfer transitions, involving the oxidation of one chromophore and reduction of another, should be approximately degenerate with $\pi\pi^*$ states of the constituent monomers. Mixing between such ionic configurations and locally excited or exciton states can lead to substantially increased dipolar character relative to monomers, and hence larger electrochromic effects. Even in the case of centrosymmetric systems, solvent-induced symmetry breaking is sufficient to produce substantial effects [10,15]. Some electro-optic data are available for the lowest electronic excited state of simple molecular dimers [9], and this suggests a trend in which the largest changes in dipole moment parallel the largest red shifts of the dimer relative to its monomeric constituents. Although electronic structure calculations are not yet reliable enough to interpret these results fully, it is interesting to investigate structurally defined, non-covalently linked chromophore aggregates such as are present in photosynthetic light-harvesting complexes *.

The bacteriochlorophyll *a* protein (BCP) from the green bacterium *Prosthecochloris aestuarii* is the best characterized BChl *a*/protein antenna complex. Its X-ray crystal structure has been determined to 1.9 Å resolution [17,18]. The complex consists of seven bacteriochlorophyll *a* (BChl *a*) molecules surrounded by protein consisting largely of extended beta-sheets. The center-to-center distances between the BChl *a* rings are 11.3–14.4 Å, and the closest edge-to-edge separation is approx. 4 Å [18]. This water-soluble protein has been extensively studied using low-temperature absorption, CD, and high-resolution derivative-absorption spectroscopies [19–22] in attempts to assign the many bands that occur in the region of the BChl *a* Q_y transitions (700–850 nm). The near-infrared absorption bands have been assigned to exciton transitions arising from inter- and intracomplex interactions among the BChl *a* monomers, and this is consistent with the conservative, split CD spectrum in this region [19]. Consequently, many attempts have been made to calculate the observed absorption and CD spectra using simple exciton theory [23,24]. Recently, more sophisticated INDO/s calculations have also been applied to this complex [25].

The B800-850 (LHII) and B875 (LHI) light-harvesting complexes from purple non-sulfur bacteria such as *Rhodobacter sphaeroides* and *Rhodobacter capsulatus* are further examples of chromophore systems where interchromophore interactions lead to very rapid and efficient intracomplex energy transfer (carotenoid → BChl *a* and BChl *a* → BChl *a*) [26–28]. If there is a simple correlation between the magnitude of the bathochromic shift in a chromophore aggregate and the dipole moment difference between the ground and excited states, $|\Delta\mu_A|$, then the 850 nm band in the B800-850 complex is expected to have a larger $|\Delta\mu_A|$ than the 800 nm band, and the transition associated with B875 should have a still larger $|\Delta\mu_A|$.

Although crystals of the B800-850 membrane-bound complex from several different photosynthetic bacteria have been prepared [29–31], no structure has yet been reported. Several structural models have been proposed for the nine chromophores (six BChl *a* and three carotenoid) in the minimal unit [32]. The two polypeptide dimers that make up the protein component (a pair of the α and β proteins) are short stretches of α-helix which leave the chromophores exposed to the surrounding solvent (presumably the hydrophobic interior of the membrane) or chromophores bound to adjacent helices [33]. Current models postulate that the 800 nm band is associated with a weakly interacting dimer of BChl *a* molecules, while the 850 nm band is due to some arrangement of four BChl *a* [32]. It has also been observed that addition of the detergent lithium dodecyl sulfate (LSD) to a solution of the complex results in nearly complete attenuation of the 800 nm band, with only small absorption changes elsewhere in the visible spectrum [34]. Subsequent dialysis to replace the LDS with lauryl dimethylamine *N*-oxide (LDAO) causes almost 100% reversal of this effect. This unusual observation is consistent with previous explanations that LDS treatment results in detergent-enhanced dissociation of the 800 nm BChl *a* chromophore; however, no other comprehensive hypothesis has been proposed.

The LHI antenna complex in purple bacteria is tightly associated with the RC [35], and, consequently, it is difficult to purify it free from RC and LHII. An expression system has been developed [36,37] for preparing RC mutants of *Rb. capsulatus* that also provides B875 with no B800-850 contamination. The B875 antenna complex from *Rb. capsulatus* has been shown to exhibit spectroscopic characteristics quite similar to the same antenna in *Rb. sphaeroides* [38]. We therefore chose to study the B875 complex in this form, and this also gives us the opportunity to extend Stark

* Parson et al. [16] have recently published calculations of the absorption spectrum for a molecular crystal of methyl bacteriopheophorbide *a* (MeBPheo *a*) using an exciton and charge-transfer interaction model. The results of this study indicate that absorption properties are very sensitive to the magnitude of the interactions of the exciton states with nearby charge-transfer transitions. Stark effect results from our laboratory on crystalline MeBPheo *a* confirm that the red-shifted Q_y absorption band does carry substantial charge-transfer character, manifest as a large difference dipole moment associated with this transition [9].

effect measurements to whole membrane preparations. Pigment determinations indicate that the minimal unit consists of a set of α/β polypeptides with significant homology to those of B800-850 associated with two BChl *a* and two carotenoid molecules [39]. Kinetic measurements of energy migration and genetic analysis have suggested a model in which B875 is intimately connected with the RC, and this is then surrounded by the more peripheral B800-850 [28]. This is consistent with a classical antenna system in which excitation energy is funneled from higher to lower energy states ultimately arriving at the special pair of the RC (P870 in *Rb. sphaeroides*). In addition to the intrinsic interest in the electronic structure of BChls in these antenna complexes, Stark effect studies for all pigmented components comprising the photosynthetic membrane provide information on the contributions from possible contaminants in absorption and especially fluorescence Stark effect measurements of wild-type and mutant RCs.

Materials and Methods

The bacteriochlorophyll *a* protein from *P. aestuarii* (strain 2K) was obtained as a kind gift from Professor Roger Fenna (University of Miami). Spectra were obtained with samples in a buffer of 0.01 M Tris and 0.2 M NaCl (pH 8.0). Low-temperature spectra were recorded using the above buffer diluted 1:1 (v/v) with glycerol. The room-temperature absorbance ratio A(809 nm)/A(371 nm) was greater than 2.3, and the UV-Vis spectrum matched those previously published [20], indicating good sample integrity. The B800-850 light-harvesting complex was obtained as a side-product of reaction center preparation (*Rb. sphaeroides* wild-type strain WS 231 kindly provided by Professor Schenk) [40]. The complex was purified using a sucrose density gradient followed by FPLC, and was then suspended in a buffer of 0.015 M Tris/1 mM EDTA/0.1% LDAO (pH 8.0). The room-temperature absorption spectrum in the Q_y region is similar to that previously reported [32]; the carotenoid region is slightly different because spheroidenone is produced, replacing some of the spheroidene, when the organisms are grown semi-aerobically [41]. A sample of B800-850 from organisms grown anaerobically was kindly provided by Carol Violette in Professor Frank's laboratory (University of Connecticut). This sample, prepared under different conditions, gives identical absorption and Stark effect results in the Q_y region. Treatment of B800-850 with LDS (Aldrich) was performed as described in the literature [42] and resulted in approx. 75% attenuation of the 800 nm absorption band. B875-containing membranes were prepared by expressing pCR, a plasmid carrying the RC and B875 genes [36], in *Rb. capsulatus* strain U43 (RC^-, LHI^-, $LHII^-$) [37], which was generously provided by Professor Youvan. The purified chromatophores were suspended in 10 mM phosphate buffer (pH 7.4). The room temperature absorption spectrum of the BChl *a* Q_y region matched that of the Ala^+ mutant ($LHII^-$, $Carotenoid^-$) of *Rb. capsulatus* [38] and that of the isolated B875 from *Rb. sphaeroides* [39] with minor differences in absorption maxima. A small amount of RC is visible as absorption at 760 and 800 nm. In order to eliminate contributions to the absorption and Stark effect spectra in the 850–900 nm region which overlaps with B875, the RC special pair was oxidized in some samples with a large molar excess of $K_3Fe(CN)_6$.

When an external electric field ($\mathbf{F}_{ext}$) is applied to a non-oriented and immobilized sample of absorbing molecules, the change in the absorption spectrum, $\Delta A(\nu)$, can often be described as a linear combination of zeroth, first and second derivatives of the absorption band, $A(\nu)$ [43]:

$$\Delta A(\nu) = \left[A_\chi \cdot A(\nu) + \frac{B_\chi}{15h} \cdot \frac{\nu \mathrm{d}(A(\nu)/\nu)}{\mathrm{d}\nu} + \frac{C_\chi}{30h^2} \cdot \frac{\nu \mathrm{d}^2(A(\nu)/\nu)}{\mathrm{d}\nu^2} \right] \cdot \mathbf{F}_{int}^2 \quad (1)$$

where h is Planck's constant, χ is the experimental angle between $\mathbf{F}_{ext}$ and the electric polarization of light at the frequency, ν, used to probe the effect, and $F_{int} = f \cdot \mathbf{F}_{ext}$, where f is the local field correction (assumed to be a scalar). Models of various levels of sophistication can be applied to estimate f, and its value is typically expected to be 1.2–1.4 for the systems reported here assuming the spherical cavity approximation [2]. Results for $|\Delta\boldsymbol{\mu}_A|$ are given in units of Debye/f to facilitate comparison. For all systems reported here, ΔA was observed to depend quadratically on the applied field strength. A_χ and B_χ are fully described elsewhere [44]; roughly, A_χ provides information on the transition moment polarizability and hyperpolarizability, and B_χ on the change in polarizability ($\Delta\boldsymbol{\alpha}$) associated with an electronic transition. $C_\chi = \{5 \, |\Delta\boldsymbol{\mu}_A|^2 + (3 \cos^2\chi - 1)[3(\mathbf{p} \cdot \Delta\boldsymbol{\mu}_A)^2 - |\Delta\boldsymbol{\mu}_A|^2]\}$, where $\mathbf{p}$ is a unit vector along the transition moment and $\Delta\boldsymbol{\mu}_A$ is the change in permanent dipole moment associated with the transition (the angle between them is ζ_A). In principle, a decomposition of the ΔA spectrum into its component derivatives with their χ-dependences provides quantitative estimates of these electro-optic properties and their projections onto $\mathbf{p}$. The variation in ζ_A for different bands can be eliminated by measuring the Stark effect at the magic angle ($\chi = 54.7°$, C_χ independent of ζ_A). The expression for electromodulated fluorescence, ΔF, is the same except that ΔF is proportional to the ν^3-weighted derivatives [45], and the subscript F is used on $\Delta\boldsymbol{\mu}$ and ζ. When multiple transitions overlap in a spectrum, the accurate

determination of the parameters $\Delta\mu$ and ζ is hindered, as each band in the ΔA or ΔF spectrum is weighted independently. In this study we calculate the parameters separately for the individual transitions, noting that overlap may result in some systematic error. As discussed further below, Eqn. 1 has often been found to be very useful, although as more complex systems are examined with better signal/noise, we find many cases where $\Delta A(\nu)$ data cannot be satisfactorily decomposed into a simple sum of derivatives. Possible origins of such behavior are discussed by Reimers and Hush [46] and Middendorf [61].

Stark, absorption, and fluorescence spectroscopies were performed on samples of frozen glycerol/buffer glasses (77 K) in cells consisting of two glass slides that had been coated with Ni electrodes on their inner surfaces (Ni thickness typically 75 Å, transmittance typically 50% per surface). The sample path length was determined by a spacer 0.10–0.12 mm thick and was measured accurately (± 5 μm) using a precision caliper. Some experiments were also performed on samples embedded in poly(vinyl alcohol) (PVA) and cast as thin films (typical thickness 50 μm) on a clean glass slide. These films were then coated with semi-transparent Ni electrodes [4]. The experimental apparatus for both absorption and fluorescence Stark effect measurements has been reported previously [2,3,7,8] and is briefly described here. Samples were cooled to 77 K in a liquid-N_2 dewar with strain-free, quartz optical windows. The applied electric field was sinusoidal with a peak-peak amplitude across the sample of up to 10^6 V/cm. Transmission and fluorescence signals were probed with a 100 W tungsten-halogen lamp passed through a 1/4 m monochromator (resolution 1.8 nm) and measured using a Si avalanche photodiode (RCA C30956E) biased at 300 V and lockin detection. Absorption (A) and fluorescence (F) spectra were measured using light chopped mechanically at 400 Hz. Electromodulated difference signals (field-on minus field-off, ΔA and ΔF spectra) were detected at the second harmonic ($2f$ typ. 650 Hz) of the applied a.c. electric field. Transmission spectra were converted to absorbance digitally (a reference transmission scan was obtained using a Ni-coated blank sample), and derivative spectra were generated by numerical differentiation of digitized experimental data. In some cases, to enhance the signal-to-noise ratio of derivatives needed for analysis, they were not obtained directly from the data. Rather, the absorption was least-squares fit to an arbitrary function (multiple higher-order Gaussian bands) and the appropriately weighted derivatives obtained from the fit. This smoothing procedure gives derivatives which are nearly identical to those obtained from the data directly, but allows one to resolve small features of the second-derivative spectrum. Polarization measurements were obtained by rotating the sample about a vertical axis while the probe light was horizontally polarized by a Glan-Thompson polarizer (see Ref. 2 for details). Methods for determining $|\Delta\mu|$ and the internally defined angle ζ from experimental data (ΔA and ΔF spectra) have been previously published [2,7].

Results

BChl a-protein

At room temperature, BCP has a broad Q_y transition with a maximum at 809 nm. As the temperature is lowered, and by 77 K, the band is resolved into at least six components as revealed by 8th-derivative spectroscopy [20]. Four of these are evident in Fig. 1A. One of the interesting features of this spectrum is the extremely narrow linewidths of the individual absorption bands compared to those of the Q_y band of in vitro BChl *a*. This has been explained as a manifestation of the exciton coupling among multiple chromophores [23]. Fig. 1B shows the Stark effect spectrum (ΔA), and this can be compared with the ν-weighted second derivative calculated from the absorption which is shown in Fig. 1C. For all four resolved bands (790,

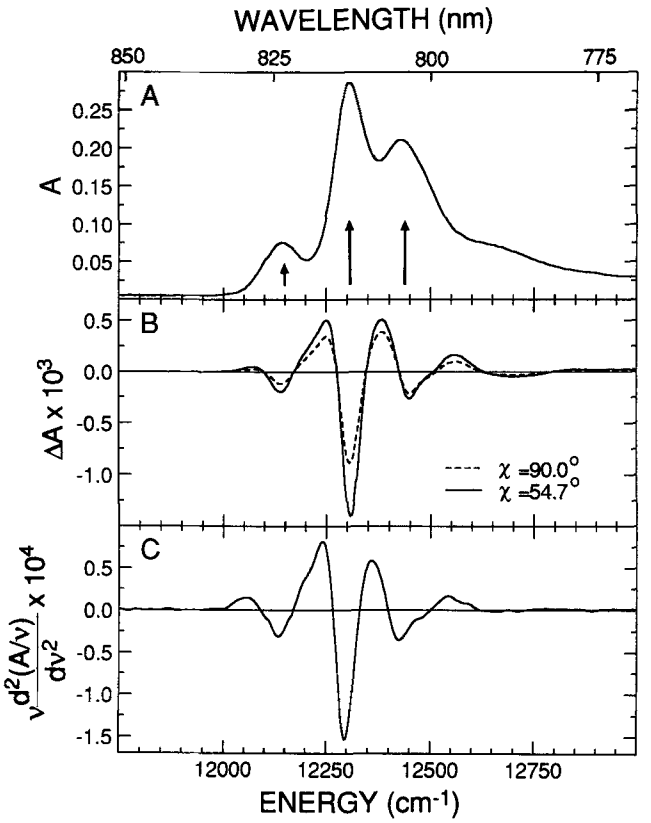

Fig. 1. (A) Absorption, (B) Stark absorption and (C) second derivative of absorption of Bacteriochlorophyll *a* protein from *Prosthecochloris aestuarii* in a glycerol/buffer glass at 77 K, $\mathbf{F}_{ext} = 2.5 \cdot 10^5$ V/cm. ΔA spectra are shown for $\chi = 90.0°$ and 54.7°, and the second derivative in (C) was obtained directly from the absorption data.

805, 813, and 824 nm) the Stark effect is proportional to the square of the applied electric field. Fig. 1B shows ΔA measured with linearly polarized light at the experimental angles $\chi = 90.0°$ and $54.7°$. Comparison of these two spectra indicates that the angle between the difference dipole $\Delta\mu_A$ and the transition dipole is very similar for all the transitions with the possible exception of the band at 805 nm. A quantitative measurement of the absolute angle ζ_A is hampered by the overlap of the various bands; however, the variation in ΔA with χ is large and positive, so ζ_A must be less than about $30°$. Even with $\chi_A = 30°$, 87% of the difference dipole is projected along the axis of the transition moment. Values of $|\Delta\mu_A|$ calculated for the individual bands using the data shown are presented in Table I. Since the calculated values of $|\Delta\mu_A|$ depend to some extent on ζ_A, and ζ_A is somewhat uncertain due to band overlap, a range of $|\Delta\mu_A|$ is given which is computed using values of the angle ζ_A over the range $0–30°$. The range of $|\Delta\mu_A|$ calculated in this manner is still smaller than the error in the measurement at any given ζ_A.

Fig. 2A shows the fluorescence spectra of BCP at 298 K and 77 K. As can be seen, there are two or more states with appreciable emission at room temperature; however, at 77 K fluorescence is primarily from the lowest energy state (absorption maximum at 824 nm) with the emission maximum at 827 nm. The Stark effect on the emission at 77 K is shown in Fig. 2B. The ΔF spectrum compares well with the ν^3-weighted second derivative of the emission shown in Fig. 2C, although there is a slight shift in the peak minimum to

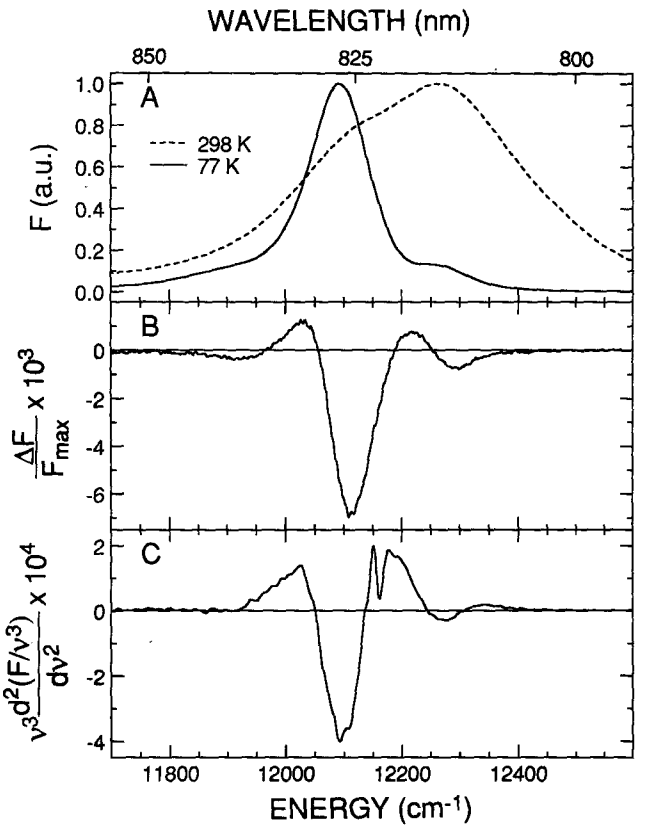

Fig. 2. (A) Fluorescence, (B) Stark fluorescence and (C) second derivative of fluorescence of Bacteriochlorophyll *a* protein from *Prosthecochloris aestuari* in a glycerol/buffer glass at 77 K, λ_{ex} = 380–520 nm, $F_{ext} = 3.0 \cdot 10^5$ V/cm. Fluorescence obtained at 298 K is also shown in (A). The ΔF spectrum shown was measured for $\chi = 90.0°$, and the second derivative in (C) was obtained directly from the fluorescence data.

TABLE I

Values of $|\Delta\mu_A|$ and ζ_A for features in the Q_y region of antenna complexes and monomeric BChl a at 77 K

Chromophore	Solvent	Absorption maximum (cm^{-1}/nm)	$\lvert\Delta\mu_A\rvert/f$ [a] (D)	ζ_A
Bacteriochlorophyll *a* protein (BCP)	glycerol/buffer	12136/824	1.3–1.5	
		12300/813	1.8–2.0	≈ 30°
		12422/805	1.8–2.0	
		12658/790	⩽ 2.8 [b]	
Rb. sphaeroides				
B800-850	glycerol/buffer	11751/851	3.1–3.4	< 30°
		12500/800	0.8–0.9	≈ 0°
	PVA	11764/850	2.8–3.1	
		12594/794	0.4–0.5	
B800-850/LDS	PVA	11641/859	3.5–4.0	
Rb. capsulatus				
B875	glycerol/buffer	11161/896	3.3 ± 0.2 [c]	13 ± 2°
Bacteriochlorophyll *a* [d]	PMMA	12853/778	2.4 ± 0.2 [c]	12 ± 2°

[a] Range given is for $\zeta_A = 0–30°$.
[b] This is an upper limit due to low signal/noise in the second derivative spectrum.
[c] Calculated using the determined value of ζ_A.
[d] Data from Ref. 4. PMMA = poly(methyl methacrylate), pyridine added as ligand so BChl is 6-coordinate and monomeric.

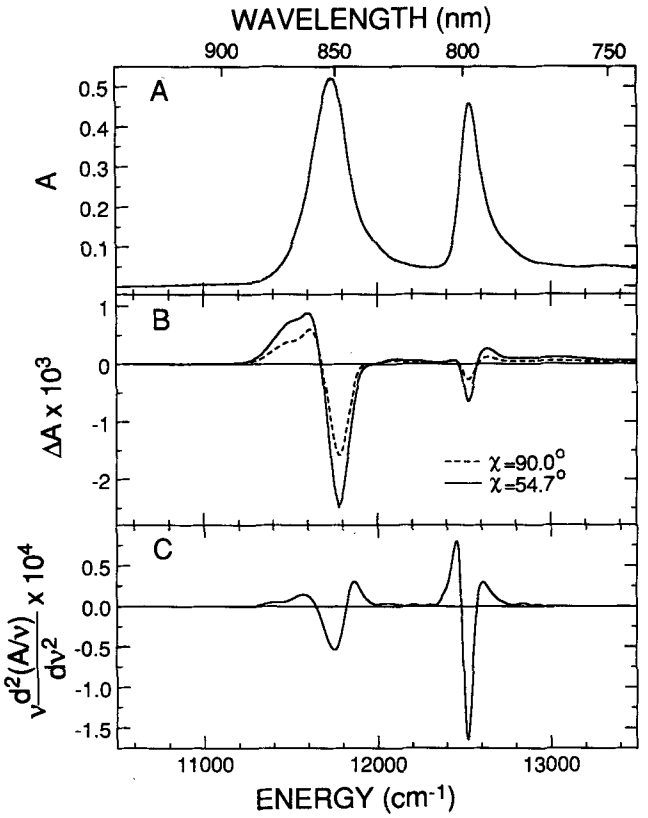

Fig. 3. (A) Absorption, (B) Stark absorption, and (C) second derivative of absorption of B800-850 light-harvesting complex from *Rhodobacter sphaeroides* in a glycerol/buffer glass at 77 K, $\mathbf{F}_{ext} = 2.8 \cdot 10^5$ V/cm. ΔA spectra are shown for $\chi = 90.0$ and 54.7°. The second derivative in (C) was obtained from a fit of the absorption between 10500 and 13000 cm^{-1} (see text for details).

826 nm. Using the values of $\Delta F/F_{max}$ at the peak minimum and the corresponding value of the second derivative at the same wavelength results in a $|\Delta\mu_F| =$ 1.6–1.8 D/f for $\zeta_F = 0$–30°.

B800-850 complex

Unlike the relatively straightforward results for BCP, those for the B800-850 complex are more complex. Fig. 3 shows the absorption, Stark effect, and second-derivative spectra of the B800-850 complex in a glycerol/buffer glass at 77 K. Due to the presence of overlapping transitions, there are unresolved features in the absorption spectrum which are revealed in the second derivative and Stark spectra. Comparison of the ΔA and second-derivative spectra shows quite clearly that the electric field effect for the 850 nm band is substantially larger than for the 800 nm band. A closer inspection reveals several anomalous features, including the positively valued shoulder on the red side of the Stark band at 850 nm. This feature has a larger magnitude of ΔA relative to its second derivative than the 850 nm band itself, indicating a larger difference dipole. This shoulder is not due to contamination from P870 of RCs, because the wavelengths of these features do not correspond [2,4]. As further proof, treatment with $Fe(CN)_6^{-3}$ to oxidize any potential trace P870 results in an absorption (as well as fluorescence) Stark effect that is essentially identical to that obtained from untreated samples. It is conceivable that the anomalous shoulder is due to overlap with the Stark effect from B875 antenna contamination; however, this is unlikely given the wavelength maximum and lineshape of the B875 Stark effect (see below). Furthermore, samples from different types of preparation and from different laboratories give identical results, suggesting that this shoulder is an intrinsic feature of the B800-850 complex.

Another anomaly in the B800-850 Stark effect spectrum is the absence of the expected positive lobes on the blue side of the 850 nm band and on the red side of the 800 nm band, seen by comparing the Stark and second-derivative spectra. Possible causes of this anomaly are discussed below. Taking the second-derivative lineshape as a first approximation and using the wavelengths at the peak minima in the Stark spectrum, calculations for the two bands give $|\Delta\mu_A|$ (851 nm) = 3.1–3.4 D/f and $|\Delta\mu_A|$ (800 nm) = 0.8–0.9 D/f for the range $\zeta_A = 0$–30° (see Table I). A more accurate determination of ζ_A is difficult due to spectral overlap and depolarization by the glycerol/buffer glass. ΔA depends strongly on χ, and a rough estimate for the 800 nm band is that $\zeta_A \approx 0°$; the value of ζ_A for the 850 nm band is somewhat larger, but is less than 30°.

The B800-850 complex was also examined in a PVA film, because the LDS-containing sample had to be studied under these conditions *. The ratio of absorption between the 850 and 800 nm bands increases from about 1.5 in glycerol/buffer to 1.9, both transitions are broadened, and the 800 nm transition is shifted to 794 nm at 77 K (data not shown). The results of calculations of $|\Delta\mu_A|$ for the two transitions in PVA films are given in Table I. While $|\Delta\mu_A|$ for the 850 nm band in PVA and a glycerol/buffer glass are nearly the same, for the 800 nm band a 50% decrease is measured. Samples of the B800-850 complex which had been treated with LDS and embedded in PVA also show only a small change in $|\Delta\mu_A|$ for the long wavelength band (see Table I), with a complete absence of any features in the Stark effect spectrum in the region of the 800 nm band (data not shown).

* In the course of these investigations we discovered that the Stark effect spectra of frozen glass samples containing ionic detergents such as LDS or SDS is completely dominated by large oscillations. The origin of these interesting oscillations is not known and is being investigated. No such oscillations are observed in frozen glasses containing non-ionic detergents such as LDAO, and they are not observed when samples containing ionic detergents are embedded in PVA films.

It is interesting to compare these results with those obtained for the Q_y transition of the special pair in *Rb. sphaeroides* reaction centers. Treating the ΔA spectrum as the second derivative of the absorption, a value of $|\Delta\mu_A| = 7.0 \pm 0.5$ D/f has been obtained at 77 K [4–6]. We have recently shown, however, that the relationship between ΔA and A for the special pair is more complex by measuring ΔA at 1.5 K in a glycerol/buffer glass [47]. Irrespective of the interpretation of these results, the special pair Q_y transition is considerably more sensitive to an applied field than the 850 nm band of the B800-850 complex.

The fluorescence and electric field modulated fluorescence from the B800-850 complex at 77 K are shown in Fig. 4. Interestingly, the 872 nm fluorescence maximum at 77 K is substantially red-shifted from the 857 nm room-tempterature maximum (data not shown), although there is little temperature dependence to the absorption peak position. The ΔF spectrum shows an unprecedented net decrease in the fluorescence intensity. This can largely be described as a negative zeroth derivative change, except for the slight blue shift of the peak maximum for ΔF relative to F (868 nm vs. 872 nm) and a narrowing of ΔF compared to F (FWHM

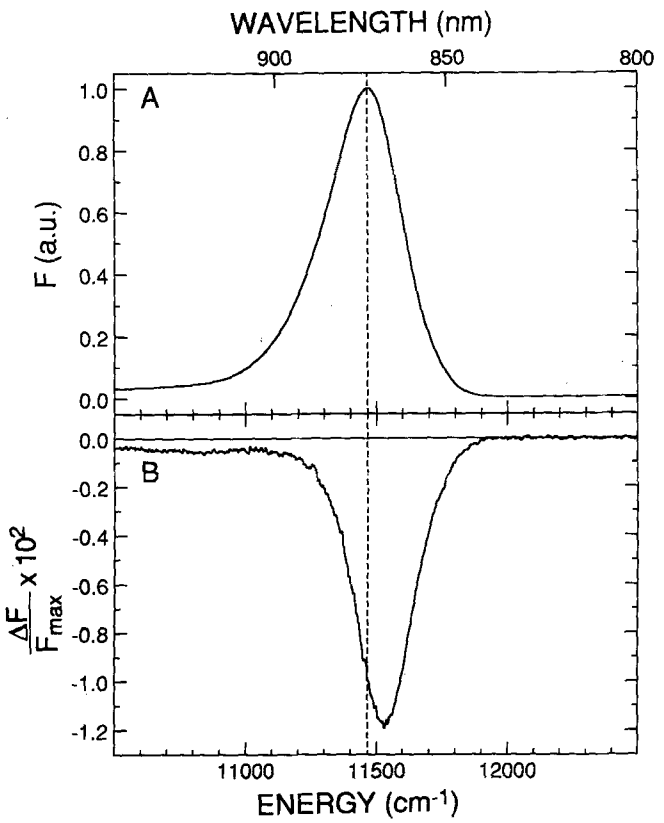

Fig. 4. (A) Fluorescence and (B) Stark fluorescence for B800-850 from *Rhodobacter sphaeroides* in a glycerol/buffer glass at 77 K, $\lambda_{ex} = 375$–500 nm, $F_{ext} = 2.6 \cdot 10^5$ V/cm. The ΔF spectrum shown was measured for $\chi = 90.0°$. Note that the ΔF scale is very different from the ΔA scale in Fig. 3B for comparable values of F_{ext}.

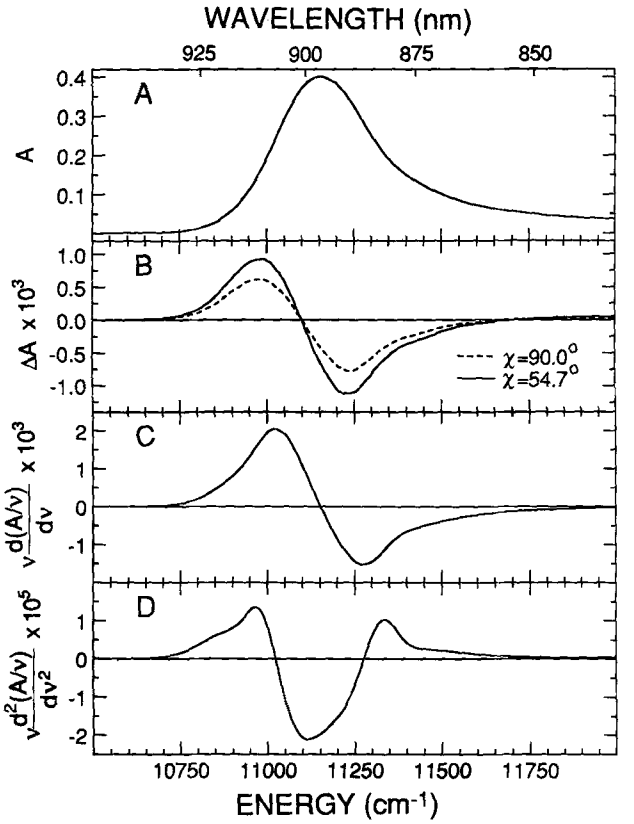

Fig. 5. (A) Absorption, (B) Stark absorption, (C) first derivative of absorption, and (D) second derivative of absorption of B875 light-harvesting complex in chromatophores of *Rhodobacter capsulatus* in a glycerol/buffer glass at 77 K. $F_{ext} = 1.9 \cdot 10^5$ V/cm. ΔA spectra are shown for $\chi = 90.0°$ and 54.7°. The derivatives in (C) and (D) were obtained from a fit of the absorption between 10500 and 12000 cm^{-1} (see text for details).

260 cm^{-1} vs. 345 cm^{-1}). The magnitude of ΔF is proportional to the square of the applied external electric field over the range (1.7 to 3.9) $\cdot 10^5$ V/cm. In addition to the unusual negative zeroth derivative lineshape, the observed change is of the magnitude that would be expected for a second-derivative change in F if $|\Delta\mu_F|$ were > 10 D/f. The reduction in fluorescence is also observed in samples embedded in PVA films, where both the F and ΔF spectra have broader linewidths than those in a glycerol/buffer glass *.

B875 complex

Stark effect results for the Q_y absorption of the B875 complex in chromatophore membranes at 77 K

* B800-850 samples were observed to photodegrade with intense excitation in the Soret region giving an overall net decrease in the fluorescence intensity with time. The shape and magnitude of $\Delta F/F_{max}$ does not, however, change as the fluorescence decreases indicating a spectrally homogeneous reduction in fluorescing chromophores. Furthermore, excitation using weaker 790–810 nm bandwidth radiation does not result in photodegradation over the course of an experiment and gives the same observed ΔF effect. See also previous footnote (p. 68).

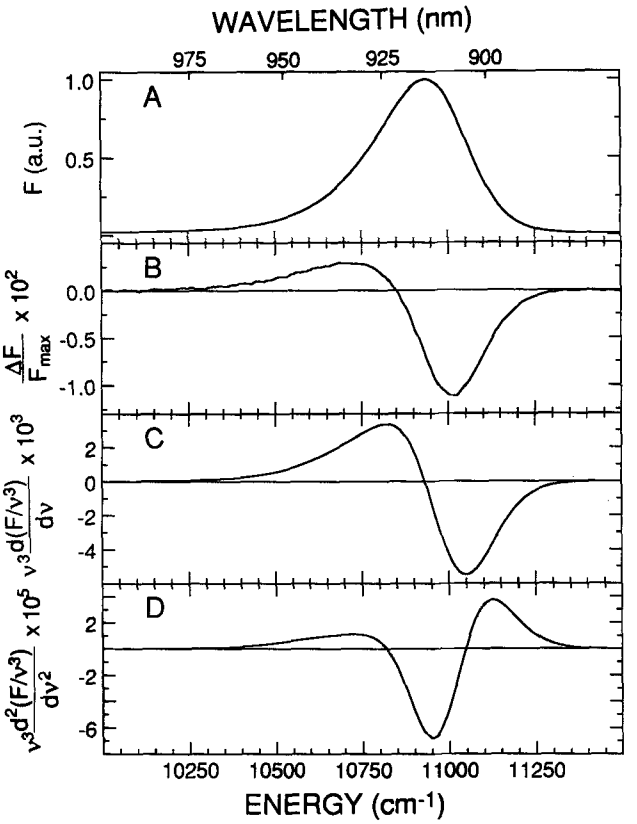

Fig. 6. (A) Fluorescence, (B) Stark fluorescence, (C) first derivative of fluorescence, and (D) second derivative of fluorescence of B875 light-harvesting complex in chromatophores of *Rhodobacter capsulatus* in a glycerol/buffer glass at 77 K, λ_{ex} = 375–500 nm, F_{ext} = 2.2·10^5 V/cm. The ΔF spectrum shown was measured for $\chi = 90.0°$.

are shown along with the first and second derivatives of the absorption band in Fig. 5. There is a shift in the absorption band maximum from the room temperature value of 883 nm to 896 nm at 77 K. The Stark effect spectrum of this complex is dominated by a contribution from the first derivative of the absorption. Fitting of the ΔA spectra obtained at different values of χ to a sum of derivative components, assuming that Eqn. 1 is appropriate, results in $|\Delta\mu_A| = 3.3 \pm 0.2$ D/f and $\zeta_A = 13 \pm 2°$. In addition, a very large polarizability difference ($|\mathrm{Tr}(\Delta\alpha)| > 1000$ Å$^3/f^2$), also with its principal axis nearly parallel to the transition moment direction, is derived based on this analysis.

The fluorescence Stark effect for B875 is shown in Fig. 6. As for the B800-850 complex, the fluorescence maximum (915 nm) is quite red-shifted from the room temperature value (903 nm), although this parallels the absorption shift in B875. The ΔF lineshape is dominated by a first-derivative component, as is evident upon visual inspection of Fig. 6 and is confirmed by fitting the Stark spectrum to a sum of derivatives as described in Eqn. 1. The fit also indicates a sizable negative zeroth derivative contribution. The overall magnitude of ΔF is quite large relative to the derivatives and corresponds to $|\Delta\mu_A| = 5.2$ D/f with $\zeta_A = 13°$ and $|\mathrm{Tr}(\Delta\alpha)|$ up to 4000 Å$^3/f^2$. It is unlikely that Eqn. 1 describes this system, and alternative explanations for the anomalous lineshapes that avoid these physically unreasonable values for the parameters are considered below.

Discussion

BChl a protein

The absorption spectrum of BCP in the Q_y region has been studied by numerous investigators [19–23], with the current consensus that the bands are due to exciton interactions among the seven chromophores in the complex. Using the crystal structure coordinates and simple exciton theory [48] to calculate the expected shifts results in rather poor agreement with the observed absorption and CD spectra [19,21,23]. The spectra can be somewhat better simulated if an arbitrary, constant shift, rationalized as an environmental effect, is added to all bands [19]. In order to perform such an analysis, it is necessary to decide which features are band origins and which are vibronic components. It seems simplest and most reasonable to us to consider the three prominent features at 824, 813, and 805 nm (77 K, glycerol/buffer glass) highlighted with arrows in Fig. 1 to be the band origins for 1, 3 and 3 BChl *a* molecules in the complex, respectively. The remaining very weak features at higher energy are taken to be vibronic bands or higher energy exciton components associated with the three origins. This assignment of bands is quite different from that considered by Pearlstein et al. [20,21,23,24], but is consistent with a recent study by Gudowska-Nowak et al. [25]. The latter work (INDO/s calculations based on the crystallographic data) indicates that skeletal flexibility of the porphyrin rings of the chromophores resulting in conformational distortions can be responsible for the observed optical properties. The structural variability is attributed to the protein environment in the form of axial ligands, substituent orientations and the effects of neighboring residues.

The electric field modulated absorption for BCP shown in Fig. 1 and the results in Table I indicate that the difference dipoles for the three prominent transitions are similar to that for an isolated monomeric BChl *a*. The Stark spectrum (Fig. 1B) is a nearly identical replica of the analytically obtained ν-weighted second derivative of the absorption (Fig. 1C). Furthermore, within the range of wavelengths scanned (700–1000 nm) no feature with a large $|\Delta\mu_A|$ that might be attributed to a charge-transfer transition is observed. The small variability in the values of $|\Delta\mu_A|$ that are observed for the bands may be attributed to the differences in intermolecular interactions among the chromophores that are associated with each transition, but

the differences are too small to analyze further. Thus, the basic result from the Stark effect measurement is that the BChl *a* molecules in BCP are essentially indistinguishable from a collection of monomer chromophores. The only anomaly is that the values of $|\Delta\mu_A|$ are slightly smaller than measured for BChl *a* monomer in PMMA (2.4 D/*f*). This difference may be due to the different local field corrections in the protein and a PMMA matrix or differences in axial ligands (the isolated BChl *a* monomer was 6-coordinate with pyridines as the ligands in order to avoid aggregation).

A recent study of persistent spectral hole-burning of BCP by Johnson and Small [49] provides information on related issues. A broad satellite hole was observed at 814 nm along with a narrow hole at 825 nm upon burning at 825 nm, and this was taken as evidence for strong exciton coupling (connectivity) between the chromophores. It is equally possible that the broad hole at 814 nm is a phonon side-band hole of the zero phonon hole at the burn wavelength. Furthermore, the narrow hole observed upon burning into the 824 nm band is also consistent with the Stark effect results which we interpret as indicating that the bands represent species with monomer-like properties. Our study of chlorophyll dimers [9] has led us to conclude that species with large difference dipoles often exhibit large changes in equilibrium nuclear geometry upon excitation which may be manifest as an anomalously broadened hole spectrum. The fact that BCP has both a narrow hole and a monomer-like difference dipole is a strong indication that coupling between the chromophores is small. This same study [9] has provided evidence that there is a correlation between the bathochromic shift of the Q_y band in this series of dimers and the difference dipole of the transition. The results presented here in conjunction with those in Ref. 49 show no such correlation, which is a further indication that the transitions of the BChl *a* in BCP are shifted from the monomer due to environmental effects rather than strong interchromophore interactions.

All antenna complexes from photosynthetic bacteria undergo efficient energy transfer from higher energy excited states (and from carotenoid excited states) to the lowest-energy BChl *a* Q_y transitions. At 77 K, these are 824 nm in BCP, 850 nm n B800-850 and 896 nm in B875. In the absence of subsequent energy transfer to other light-harvesting complexes or to the reaction center, fluorescence occurs from these lowest-energy excited states with a relatively large quantum yield (0.29 for BCP [50], 0.23 for B800-850, and 0.17 for B875 [39] at 77 K). Interestingly, at room temperature, radiative relaxation occurs from at least the two lowest excited states of BCP, as the energy level difference is comparable to the thermal energy. As the temperature is lowered to 77 K, the emission is primarily from the lowest energy state [51]. This explanation of the temperature dependence of the fluorescence spectrum is also applicable to the B800-850 and B875 complexes (see below).

The electric-field-modulated fluorescence of BCP at 77 K is seen to be similar in shape to the ν^3-weighted second derivative of the emission band (Figs. 2B and 2C) [45]. The slight shift and linewidth change may be due to the presence of small first and/or zeroth derivative components as has been observed in other systems [7,8]. A small negative zeroth-derivative contribution (due to a change in the fluorescence quantum yield in the electric field, for example) would reduce the size of the positive lobes and broaden the negative lobe of the Stark spectrum, as is observed. As this is a small component, its effects were ignored for the analysis of $|\Delta\mu_F|$. The basic result is that $|\Delta\mu_F| \approx |\Delta\mu_A|$, which indicates that the electronic states whose difference dipoles are measured in absorption and fluorescence are probably the same. These results serve to confirm those found in absorption, that the BCP complex consists of loosely coupled, monomer-like chromophores, where the differences in transition energy relative to that of a BChl *a* monomer are due largely to environmental effects rather than strong excitonic interactions. Furthermore, although energy transfer is efficient, there is no evidence that the electric field affects the rate of energy transfer, as the amplitude and shape of the fluorescence would be expected to change substantially (possibly not unlike the effect of temperature). Thus, unlike CD which is exquisitely sensitive to weak, quite long-range, chiral interactions, the Stark effect is primarily sensitive to strong intermolecular interactions where the chromophore separation is quite small.

B800-850 complex

The absorption Stark effect spectrum of B800-850 in a glycerol/buffer glass (as well as in a PVA film) shows several interesting deviations from the experimentally obtained second derivative spectrum (Fig. 3). In contrast to BCP, the ΔA spectrum does not match the second derivative spectrum in many details. Primarily, the spectral region between the 800 and 850 nm bands does not mirror the gross features seen in the second derivative spectrum. It is possible that there are contributions to the electromodulated spectrum from the zeroth and/or first derivatives of the absorption bands which could conspire to produce the observed lineshape. The absorption of the 850 nm band can be modeled as a sum of higher-order Gaussian bands, and the observed Stark spectrum can be fit to a combination of zeroth, first and second derivatives. The best fit partially reproduces the observed $\Delta A(\nu)$ lineshape, but fails to fully fit the entire spectrum. In addition, it cannot model the feature to the red of the 850 nm

band without so many fitting parameters as to make the results physically unreasonable. A second explanation for the anomalous lineshape may be that there is a distribution of difference dipoles across the absorption band with those chromophores contributing to the blue and red edges of the 850 and 800 nm bands, respectively, having $|\Delta\mu_A| \approx 0$. This would reduce the Stark effect from those regions of the spectrum and would produce the observed lineshapes; however, no evidence for such a heterogeneity of both absorption bands has been previously presented.

The additional feature observed to the red of the 850 band in the B800-850 Stark spectrum (in both glycerol/buffer and PVA) is equally puzzling. Ferricyanide treatment does not affect the shape or magnitude of this or any other feature in the spectroscopic (absorption, fluorescence and Stark effect) results of B800-850. This rules out contamination by P870, and the shoulder does not resemble the ΔA spectrum of B875. Another explanation is that this additional band results from the Stark effect of a nearly degenerate exciton state which is buried within the inhomogeneously broadened absorption band in zero electric field, but is revealed in the second-derivative spectrum and is further enhanced in the Stark effect spectrum. In fact, two exciton components have been resolved (852 and 867 nm) using linear dichroism measurements of B800-850 in a stretched film [52]. Furthermore, Gaussian deconvolution of both the 850 nm Q_y transition in B800-850 and the Q_y transition of B875 in intact membranes of *Rb. sphaeroides* mutants reveal long-wavelength components ($BChl_{870}$ and $BChl_{896}$, respectively) that may be due to association of the antenna complexes [53]. These spectral forms of BChl *a* have been considered to be intermediates in the funneling of excitation energy from antenna to antenna and from antenna to the RC. The existence of such species may also have interesting ramifications for the analysis of the fluorescence data (see below). Recent results on strongly coupled porphyrin dimers [54] have also demonstrated that new bands appear at lower energy than the monomer Q_y transition, and these transitions can not be fully explained by exciton interactions. It was suggested that such bands may be due to mixing of exciton and charge resonance states [54], and such a mechanism may be operative here as well.

Even though the anomalous band shape makes calculation of $|\Delta\mu_A|$ for the bands problematic, to a first approximation we can treat the Stark effect spectrum as a pure second derivative to obtain estimates for $|\Delta\mu_A|$ (Table I). The 850 nm band has a $|\Delta\mu_A|$ which is larger than that found for BChl *a* monomers while the 800 nm band has a $|\Delta\mu_A|$ which is considerably smaller. This appears to be consistent with the correlation between the red shift of the Q_y transition and $|\Delta\mu_A|$ for multi-chromophore chlorophyll aggregates [9]. The BChl *a* chromophores associated with the 850 nm band are strongly coupled with an enhancement of $|\Delta\mu_A|$ similar to that found for some synthetic chlorophyll dimers [9] and the special pair of the bacterial RC [2–6]. The physical origin of this increase may be that significant charge-transfer character is mixed into the exciton states of this transition. Conversely, the transition associated with the 800 nm band has nearly zero change in dipole moment upon excitation, as is expected for a very weakly coupled system with little charge-transfer character in the excited state. Certain dimer configurations have also been observed to have difference dipole moments that are smaller than those found for the component monomers [9], and the orientation of the monomers involved appears to play a prominent role in determining $|\Delta\mu_A|$.

One possible explanation to account for some of the observed effects is that the 800 nm band is due to interactions between molecules in different minimal units of the light harvesting complex which produce a weakly coupled exciton state exhibiting a small difference dipole. It can be argued that the observed attenuation of this band upon LDS treatment is due to isolation of the individual minimal units *; however, any attempt to explain the effects of LDS treatment is burdened with the mystery of what happens to the oscillator strength of the 800 nm band. A similar model has been proposed by Scherz and Parson [55] to account for the circular dichroism observed for the 850 nm band. Their model assigns the 800 nm band to an environmentally red-shifted monomer BChl *a*. The present work and previous studies of the effect of LDS treatment on this transition seem to indicate, however, that this is not a complete explanation. Further evidence is provided by the observed effect on the Stark spectrum of changing the external medium. The spectrum in PVA compared to glycerol shows a marked change in $|\Delta\mu_A|$ for the 800 nm band, while a relatively small change is seen for the 850 nm band. This again indicates that the components associated with the 800 nm band are more susceptible to external perturbation.

The B800-850 complex exhibits a considerable shift in the zero applied field emission maximum with decreasing temperature. This may be analogous to what is observed in BCP which is the result of a change in the population of the emitting state as a function of temperature. At 77 K, we can assign the fluorescence to the long wavelength $BChl_{870}$ component described earlier, while at room temperature, thermal population results in emission from a distribution of the higher

* The effect of LDS on the Stark absorption of the carotenoid bands in the B800-850 complex [10] also indicates that the local protein environment is perturbed by treatment with the detergent.

and lower energy components [51]. The Stark effect on the emission at 77 K is a net reduction in the overall amplitude (quantum yield). A small contribution from second- and/or first-derivative effects may be responsible for the narrowing and blue shift of the Stark spectrum compared to a purely negative zeroth derivative of the emission lineshape. Furthermore, the magnitude of the difference spectrum, if it were purely a second-derivative effect, would correspond to a difference dipole of at least 10 D/f; this is 3-times larger than that expected for the main absorption band at 850 nm.

In general, when a process whose rate and/or quantum yield is sensitive to electric field competes with emission, unusual ΔF amplitudes and lineshapes, the latter not describable by sums of derivatives, can result [56]. For RCs, electron transfer competes with fluorescence and the rate of electron transfer is expected to depend on electric field [7,8]; however, for B800-850, where no reactions are documented except energy transfer, some other mechanism must be present. A possibility is that in an electric field enhanced excitation transfer or state mixing occurs that couples the initial excited state to a nearby state. In order to give a reduction in the fluorescence, this second state must possess rapid non-radiative decay routes and thus effectively reduce the overall fluorescence quantum yield. The lack of any significant zeroth derivative contribution in the Stark absorption (ΔA) spectrum of B800-850 indicates that the fluorescence decrease is unlikely due to an electric field sensitive non-radiative relaxation rate from the initially prepared excited state. It is more probable that the radiating state communicates with other states which have significant non-radiative decay pathways. If this communication is dependent on the magnitude of the electric field, then a field-dependent fluorescence quantum yield will result. Although the specific identity of the communicating state is unknown, it is possible that the previously proposed different spectral components within the 850 nm band, whose resolution is enhanced in the absorption Stark effect spectrum, are responsible. In particular, if the red shoulder is assigned to a CT state with appreciable change in dipole moment upon excitation, then the energy of this state will be very dependent on an electric field and mixing with nearby states is more likely.

The above mechanism, although not proven by the evidence presented here, is consistent with a variety of results. For example, fluorescence quenching is observed in chromatophores of *Rb. sphaeroides* upon addition of diaminodurene that affects cyclic electron flow [57]. It is postulated that light-induced proton uptake in the treated chromatophores results in an internal electric field gradient across the membrane, producing the same sort of fluorescence Stark effect as observed here for an isotropic sample due to an external electric field. Further precedents for the proposed mechanism are found in Stark effect experiments on the inorganic complex Ru(bipyridine)$_3$ (Oh, D.H. and Boxer, S.G., unpublished data) and in gas-phase measurements of formaldehyde electric field effects [58]. In the latter, electric field induced shifts in the energies of the radiative and non-radiative states results in a sharp reduction of the fluorescence quantum yield when resonance of the states is reached.

B875 complex

Many of the comments made regarding the B800-850 antenna complex above are also applicable to the B875 antenna complex. Although the lineshapes of the absorption and fluorescence Stark effects are somewhat anomalous, the absence of a change in the observations upon treatment with ferricyanide rules out the possibility that contamination by RCs is affecting the measurements. The weak, non-conservative circular dichroism signal observed for the B875 Q_y transition [59] has been interpreted to mean that the BChl *a* chromophores associated with the complex interact less than those in the 850 nm band of B800-850 where the CD is about 4 times larger and shows a conservative, split CD lineshape characteristic of exciton interaction [32]. A $|\Delta\mu_A|$ that is much smaller than expected for a species with such a large red shift (cf. the P870 special pair of *Rb. sphaeroides* with $\lambda_{max} = 874$ nm and $|\Delta\mu_A| = 7\ D/f$) is consistent with a weakly interacting pair of molecules. If this quantitative interpretation is accurate then this is a clear exception to the previously discussed correlation between bathochromic shift and $|\Delta\mu_A|$ for the Q_y transitions in many dimer complexes. If strong inter-chromophore coupling is not responsible, then, as discussed for BCP, skeletal flexibility and protein-induced structural distortion are the likely origins of the large red shift [25].

Interpretation of the Stark fluorescence results of B875 is made difficult by the magnitude and lineshape of the effect. Direct application of Eqn. 1 produces physically unreasonable values of $|\Delta\mu_A|$ and $|\mathrm{Tr}(\Delta\alpha)|$ given the other information available. In general, breakdown of the applicability of Eqn. 1 is possible when multiple transitions overlap in a single absorption or fluorescence band, as is the case for B800–850 and B875. It is also possible for forbidden transitions which are sensitive to the perturbation of the electric field to exert an effect on the Stark spectrum, even though no evidence of the transition is apparent in the zero-field spectrum. When these individual transitions have different values of the electro-optic parameters then one expects that the Stark effect can not be fit with a simple sum of derivatives of the overall band, but will require a more complicated model to assign the underlying electronic structure. Reimers and Hush [46] have

also considered a vibronic coupling mechanism to account for some of the non-classical Stark effects observed in certain coupled inorganic complexes [60]. Their theory treats the problem where not only the energies of the transitions are affected by the electric field, but also the lineshapes, due to a dependence of the electro-optic parameters on nuclear coordinate. In the case of the antenna complexes studied here, the observed anomalies in the Stark effect results further serve to indicate the complexity of the intermolecular interactions and the electronic states involved [61].

Acknowledgments

The authors thank Professors Fenna and Frank for kindly providing samples and Carol Violette for helpful discussions about sample purification. We also thank Professors Schenk and Youvan for providing bacterial strains used in this work. J.W.S. is an NSF Pre-doctoral fellow. This research was funded by the NSF Biophysics Program.

References

1 DeLeeuv, D., Malley, M., Butterman, G., Okamura, M.Y. and Feher, G. (1982) Biophys. Soc. Abstr. 37, p. 111a.
2 Lockhart, D.J. and Boxer, S.G. (1987) Biochemistry 26, 664–668.
3 Boxer, S.G., Lockhart, D.J. and Middendorf, T.R. (1987) Springer Proc. Phys. 20, 80–90.
4 Lockhart, D.J. and Boxer, S.G. (1988) Proc. Natl. Acad. Sci. USA 85, 107–111.
5 Lösche, M., Feher, G. and Okamura, M.Y. (1987) Proc. Natl. Acad. Sci. USA 84, 7537–7541.
6 Lösche, M., Feher, G. and Okamura, M.Y. (1988) in The Photosynthetic Bacterial Reaction Center – Structure and Dynamics (Breton, J. and Vermeglio, A., eds.), pp. 151–164, Plenum, New York.
7 Lockhart, D.J. and Boxer, S.G. (1988) Chem. Phys. Lett. 144, 243–250.
8 Lockhart, D.J., Goldstein, R.F. and Boxer, S.G. (1988) J. Chem. Phys. 88, 1408–1415.
9 Gottfried, D.S. (1990), Ph.D. Thesis, Stanford University.
10 Gottfried, D.S., Steffen, M.A. and Boxer, S.G. (1991) Biochim. Biophys. Acta 1059, 76–90.
11 Sebastian, L., Weiser, G. and Bässler, H. (1981) Chem. Phys. 61, 125–135.
12 Sebastian, L., Weiser, G., Peter, G. and Bässler, H. (1983) Chem. Phys. 75, 103–114.
13 Petelenz, B., Petelenz, P., Shurvell, H.F. and Smith, V.H., Jr. (1987) Chem. Phys. Lett. 133, 157–161.
14 Petelenz, P., Siebrand, W. and Zgierski, M.Z. (1988) Chem. Phys. Lett. 147, 430–434.
15 Liptay, W., Wortmann, R., Bohm, R. and Detzer, N. (1988) Chem. Phys. 120, 439–448.
16 Parson, W.W., Creighton, S. and Warshel, A. (1989) J. Am. Chem. Soc. 111, 4277–4284.
17 Matthews, B.W., Fenna, R.E., Bolognesi, M.C., Schmid, M.F. and Olson, J.M. (1979) J. Mol. Biol. 131, 259–285.
18 Tronrud, D.E., Schmid, M.F. and Matthews, B.W. (1986) J. Mol. Biol. 188, 443–454.
19 Philipson, K.D. and Sauer, K. (1972) Biochemistry 11, 1880–1885.
20 Whitten, W.B., Nairn, J.A. and Pearlstein, R.M. (1978) Biochim. Biophys. Acta 503, 21–262.
21 Whitten, W.B., Olson, J.M. and Pearlstein, R.M. (1980) Biochim. Biophys. Acta 591, 203–207.
22 Olson, J.M., Ke, B. and Thompson, K.H. (1976) Biochim. Biophys. Acta 430, 524–537.
23 Pearlstein, R.M. and Hemenger, R.P. (1978) Proc. Natl. Acad. Sci. USA 75, 4920–4924.
24 Pearlstein, R.M. (1988) in Organization and Function of Photosynthetic Antennas (Scheer, H. and Schneider, S., eds.), pp. 555–566, Walter de Gruyter, Berlin.
25 Gudowska-Nowak, E., Newton, M.D. and Fajer, J. (1990) J. Phys. Chem. 94, 5795–5801.
26 Trautman, J.K., Shreve, A.P., Violette, C.A., Frank, H.A., Owens, T.G. and Albrecht, A.C. (1990) Proc. Natl. Acad. Sci. USA 87, 215–219.
27 Shimada, K., Mimuro, M., Tamai, N. and Yamazaki, I. (1989) Biochim. Biophys. Acta 975, 72–29.
28 Bergström, H., Van Grondelle, R. and Sundström, V. (1989) FEBS Lett. 250, 503–508.
29 Allen, J.P., Theiler, R. and Feher, G. (1985) in Antennas and Reaction Centers of Photosynthetic Bacteria (Michel-Beyerle, M.E., ed.), pp. 82–84, Springer, Berlin.
30 Cogdell, R.J., Woolley, K., Mackenzie, R.C., Lindsay, J.G., Michel, H., Dobler, J. and Zinth, W. (1985) in Antennas and Reaction Centers of Photosynthetic Bacteria (Michel-Beyerle, M.E., ed.), pp. 85–87, Springer, Berlin.
31 Mantele, W., Steck, K., Wacker, T. and Welte, W. (1985) in Antennas and Reaction Centers of Photosynthetic Bacteria (Michel-Beyerle, M.E., ed.), pp. 88–91, Springer, Berlin.
32 Kramer, H.J.M., Van Grondelle, R., Hunter, C.N., Westerhuis, W.H.J. and Amesz, J. (1984) Biochim. Biophys. Acta 765, 156–165.
33 Zuber, H. (1986) Trends Biochem. Sci. 11, 414–419.
34 Clayton, R.K. and Clayton, B.J. (1981) Proc. Natl. Acad. Sci. USA 78, 5583–5587.
35 Zuber, H. (1985) Photochem. Photobiol. 42, 821–844.
36 Taguchi, A.K., Woodbury, N.W. Stocker, J.W. and Boxer, S.G. (1990) in Current Research in Photosynthesis (Baltscheffsky, M., ed.), pp. II.4.165–168, Kluwer, Durdrecht.
37 Youvan, D.C., Isamil, S. and Bylina, E.J. (1985) Gene 38, 19–30.
38 Bolt, J.D., Sauer, K., Shiozawa, J.A. and Drews, G. (1981) Biochim. Biophys. Acta 635, 535–541.
39 Broglie, R.M., Hunter, C.N., Delepelaire, P., Niederman, R.A., Chua, N.-H. and Clayton, R.K. (1980) Proc. Natl. Acad. Sci. USA 77, 87–91.
40 Hammes, S.L., Mazzola, L., Boxer, S.G., Gaul, D.F. and Schenck, C.C. (1990) Proc. Natl. Acad. Sci. USA 87, 5682–5686.
41 Cogdell, R.J. and Crofts, A.R. (1978) Biochim. Biophys. Acta 502, 409–416.
42 Chadwick, B.W., Zhang, C., Cogdell, R.J. and Frank, H.A. (1987) Biochim. Biophys. Acta 893, 444–451.
43 Liptay, W. (1974) in Excited States (Lim, E.C., ed.), pp. 129–229, Academic Press, New York.
44 Mathies, R.A. (1974), Ph.D. Thesis, Cornell University.
45 Baumann, W. and Bischoff, H. (1985) J. Mol. Struct. 129, 125–136.
46 Reimers, J.R. and Hush, N.S. (1990) Proceedings of the NATO Conference on Inorganic Spectroscopy, in press.
47 Mazzola, L.T., Middendorf, T.R., Boxer, S.G., Gaul, D. and Schenck, C.C. (1991) Biophys. J. 59, 139a.
48 Kasha, M., Rawls, H.R. and El-Bayoumi, M.A. (1965) Pure Appl. Chem. 11, 371–392.
49 Johnson, S.G. and Small, G.J. (1989) Chem. Phys. Lett. 155, 371–375.
50 Olson, J.M. (1966) in The Chlorophylls (Vernon, L.P. and Seely, G.R., eds.), p. 417, Academic Press, New York.
51 Kramer, H.J.M., Pennoyer, J.D., Van Grondelle, R., Westerhuis, W.H.J., Niederman, R.A. and Amesz, J. (1984) Biochim. Biophys. Acta 767, 335–344.
52 Bolt, J. and Sauer, K. (1979) Biochim. Biophys. Acta 546, 54–63.

53 Van Dorsen, R.J., Hunter, C.N., Van Grondelle, R., Korenhof, A.H. and Amesz, J. (1988) Biochim. Biophys. Acta 932, 179–188.
54 Bilsel, O., Rodriguez, J., Holten, D., Girolami, G.S., Milam, S.N. and Suslick, K.S. (1990) J. Am. Chem. Soc. 112, 4075–4077.
55 Scherz, A. and Parson, W.W. (1986) Photosynth. Res. 9, 21–32.
56 Lockart, D.J., Hammes, S.L., Franzen, S. and Boxer, S.G. (1991) J. Phys. Chem. 95, 2217–2226.
57 Sherman, L.A. and Cohen, W.S. (1972) Biochim. Biophys. Acta 283, 54–66.
58 Lin, S.H., Boeglin, A., Dai, H.L. and Schlag, E.W. (1988) J. Phys. Chem. 92, 5398–5404.
59 Bolt, J.D., Hunter, C.N., Niederman, R.A. and Sauer, K. (1981) Photochem. Photobiol. 34, 653–656.
60 Oh, D.H., Sano, M. and Boxer, S.G. (1991) J. Am. Chem. Soc., in press.
61 Middendorf, T.R. (1991) Ph.D. Thesis, Stanford University.